Published in final edited form as:
Cytometry A. 2011 October ; 79(10): 834–847. doi:10.1002/cyto.a.21127.

In vivo multispectral photoacoustic and photothermal flow cytometry with multicolor dyes: a potential for real-time assessment of circulation, dye-cell interaction, and blood volume

Mikhail A. Proskurnin[1], **Tatyana V. Zhidkova**[2], **Dmitry S. Volkov**[1], **Mustafa Sarimollaoglu**[3], **Ekaterina I. Galanzha**[3], **Donald Mock**[4], and **Vladimir P. Zharov**[3,*]

[1]Chemistry Department, M.V. Lomonosov Moscow State University, Moscow, Russia

[2]Faculty for Basic Medicine, M.V. Lomonosov Moscow State University, Moscow, Russia

[3]Phillips Classic Laser and Nanomedicine Laboratories, University of Arkansas for Medical Sciences, Little Rock, Arkansas 72205, USA

[4]Department of Biochemistry and Molecular Biology, University of Arkansas for Medical Sciences, Little Rock, Arkansas 72205, USA

Abstract

Recently, photoacoustic (PA) flow cytometry (PAFC) has been developed for *in vivo* detection of circulating tumor cells and bacteria targeted by nanoparticles. Here, we propose multispectral PAFC with multiple dyes having distinctive absorption spectra as multicolor PA contrast agents. As a first step of our proof-of-concept, we characterized high-speed PAFC capability to monitor the clearance of three dyes (ICG, MB, and TB) in an animal model *in vivo* and in real time. We observed strong dynamic PA signal fluctuations, which can be associated with interactions of dyes with circulating blood cells and plasma proteins. PAFC demonstrated enumeration of circulating red and white blood cells labeled with ICG and MB, respectively, and detection of rare dead cells uptaking TB directly in bloodstream. The possibility for accurate measurements of various dye concentrations including CV and BG were verified *in vitro* using complementary to PAFC photothermal (PT) technique and spectrophotometry under batch and flow conditions. We further analyze the potential of integrated PAFC/PT spectroscopy with multiple dyes for rapid and accurate measurements of circulating blood volume without *a priori* information on hemoglobin content, which is impossible with existing optical techniques. This is important in many medical conditions including surgery and trauma with extensive blood loss, rapid fluid administration, transfusion of red blood cells. The potential for developing a robust clinical PAFC prototype that is, safe for human, and its applications for studying the liver function are further highlighted.

[*]Correspondence to: V.P. Zharov, Phillips Classic Laser and Nanomedicine Laboratories, University of Arkansas for Medical Sciences, Little Rock, Arkansas 72205, USA. ZharovVladimirP@uams.edu.

Keywords

in vivo flow cytometry; photoacoustic method; photothermal spectroscopy; circulating blood volume; contrast agent; dye

INTRODUCTION/BACKGROUND

In vivo flow cytometry

Conventional flow cytometry is a powerful biological tool in which objects in blood are enumerated based on multiple characteristics (e.g., size and presence of various molecules such as antigens and types of hemoglobin). Most common techniques for assessing these characteristics are light scattering and laser-induced fluorescence of dyes coupled with antibodies (1). This accurate, high-throughput technology provides rapid multiparameter quantification of the biological properties of cells at subcellular and molecular levels, including their functional states, morphology, composition, proliferation, and protein expression. However, flow cytometry has some limitations: (*i*) extraction and processing of the cells for flow cytometric examination may alter cell properties; (*ii*) removal the cells from blood prevents the long-term study of individual cells in their native biological environment; (*iii*) flow cytometry usually requires time-consuming (hours) preparation procedures; and (*iv*) flow cytometric characterization the *in vitro* requires discontinuous sampling at limited, discrete time points.

These shortcomings could be addressed by the development of flow cytometry that allows for continuous, noninvasive assessment of events *in vivo* (2–25). However, adaptation of current *in vitro* technologies to *in vivo* observation of cells flowing in individual blood vessels faces many challenges. These include light scattering, autofluorescence, and absorption by blood and surrounding tissues, as well as multiple cell files in vessel cross-sections. Fluorescent techniques in animal models have shown promise in detection of labeled hematopoietic stem cells, GFP expressing cells, and circulating tumor cells (18–24). Nevertheless, translation of this technology to humans can be problematic due to cytotoxicity of fluorescent tags, and capabilities to assess only superficial 50–100 μm diameter microvessels with slow flow rates and depths below 200 μm.

To overcome these limitations, we proposed *in vivo* flow cytometry with PT (3,4), PA (5–8,12–14,26), Raman (14,15) and scattering (27) detection techniques. The PT and PA flow-cytometry techniques (PTFC and PAFC, respectively) are based on non-radiative transformation of the absorbed laser energy into heat and acoustic waves caused by the fast thermal expansion of the heated sample. These phenomena are monitored either through the changes in optical characteristics that are detected by a probe beam (in PTFC) or by an ultrasound transducer attached to the sample (in PAFC). Most promising for *in vivo* applications, PAFC uses either the label-free detection of cells with intrinsically light-absorbing chromophores (e.g., hemoglobin, melanin, or cytochromes) or cell labeling with strongly absorbing dyes or nanoparticles as PA molecular probes. We demonstrated the capacity of this completely noninvasive or minimally invasive approach to be used *in vivo* for (*i*) real-time monitoring of white blood cells (WBCs) in different functional states (e.g.,

normal, apoptotic, and necrotic) and (*ii*) real-time detection and enumeration of circulating tumor cells (melanoma, breast, squamous), bacteria (e.g., *E. coli* and *S. aureus*), and various nanoparticles and dyes (e.g., ICG, EB, or Lymphazurin) in blood and lymph (4,6–8,12–14,26,28). However, PTFC/PAFC have been used with single dyes that limited their capacity for multiparameter and multicolor measurements. Here, we extend their application for simultaneous, real-time assessment of several dyes. Among many potential applications the measurement of circulating blood volume (CBV) is proposed.

Circulating blood volume measurements

Accurate rapid determination of CBV is required in many clinical applications (29–33). These applications include: (*i*) evaluation of outpatients and inpatients experiencing extensive blood loss (34) and their response to therapy including rapid fluid administration and transfusion of whole blood and packed red blood cells (RBCs) (30); (*ii*) estimation of hemodilution during cardiac surgery that requires cardiopulmonary bypass but precludes blood transfusion (35,36); (*iii*) monitoring total blood loss during surgery or hemodialysis (37); (*iv*) measurement of total circulating RBC mass preoperatively and in response to erythropoietic therapies (38); and (*v*) estimation of the requirements of cardiac-assist devices (39) to support patients, especially whenever judging adequacy of CBV based on the arterial pressure is known to be inaccurate. However, existing techniques and assays are not fully suitable for these applications. The limitations of these techniques include inaccuracies, high labor requirements, and slow cycle times for initial and repeat measurements.

Some existing methods for CBV assessment are based on optical (40–43) or other methods (44–46) for *in vitro* measurement of the hemoglobin (Hb) concentration and hematocrit (Ht). The Hb concentration ([Hb]) correlates poorly with CBV and circulating RBC volume, especially in low birth weight infants and during rapid blood loss. Other existing methods for CBV assessment are based on the dilution of tags: optical dyes (47–50), fluorescent dyes (51,52) or radioactive isotopes linked to macromolecules (53,54). One of the first methods was photometric dye-dilution CBV estimation *in vitro*. The label is injected into the bloodstream and attaches itself to albumin molecules or RBCs (40–43,48). The dye concentration in a bloodstream diminishes due to dilution. Its average concentration is measured with an optical photometer in sampled blood as a change in the absorbance at a certain wavelength. The most widespread is Evans Blue dye (47). Photometric procedures are also based on similar labels in plasma (49,50) or serum (55) with predetermined Ht value (56). Photometric methods cannot be used for rapid tests with no *a priori* data on hemoglobin or Ht and are insensitive. Isotopic dilution methods are similar in principle with photometric, but specially predesigned radioactive labels are injected into the bloodstream and the average radioisotope concentration is measured *in vitro* or *in vivo* as radioactivity rather than optical absorbance. These procedures can be used in stationary clinical analysis only and relatively expensive. Radio-iodinated serum albumin (RISA) is a similar method using ^{131}I pre-tagged to albumin (57,58). RISA was found to undergo too rapid intravascular disappearance than other labels, thus making repetitive measurements difficult to perform accurately as dilution curves are not reproducible (48,59). Isotopic dilution methods are also based on the dilution of proteins or RBCs labeled with ^{51}Cr (53,60–64), ^{32}P (52,65–71) or ^{59}Fe (72–75). A technique using fluorescence-labeled albumin is based on the

abovementioned principle, but the dilution curve is measured as a fluorescence signal (51), and it has the same problems as abovementioned tag methods. Tagged transfusion methods like radioactive ^{51}Cr tagging of RBCs require an infusion of labeled RBCs (54). Indicator disappearance can be estimated by measuring a decay curve, and these measurements are fairly accurate because the material is maintained within the intravascular space, as it does not permeate the capillary wall. Similar methods of Hb subtype analysis and albumin dilution measure *in vitro* pre- and post-transfusion concentrations of Hb subtypes or albumin levels, respectively (76), then CBV is calculated from their changes (77). In current practice, most clinicians would agree that the transfusion of donor blood should be avoided unless necessary, thus making tagged transfusion methods less practical.

Recently, optical CBV clinical measurements are implemented as *in vivo* pulse dye densitometry (PDD) (35,78,79). This method is based on the principles of pulse oximetry and a dye-dilution technique with ICG (78,80–87). ICG is safely cleared by kidneys (37), and new measurements are possible every 20–30 min (after the ICG concentration from the previous injection becomes negligible). PDD provides for a rapid, semi-noninvasive and convenient bedside assessment of CBV that is applicable clinically (88–90) even for critically ill patients (91). PDD is currently widely used in pre- and post-operational periods for diagnostics of patients blood losses, and liver, gastroenterological, and cardiac diseases (35, 36, 82, 93, 92-96) adults, PDD is used for CBV determination for children and infants (32,97). PDD has significant correlation with RISA and ^{51}Cr because the distribution spaces are similar (37,98,99), correlates more or less well with other methods (thermodilution (36,79,100,101) and electrical impedance cardiography (102,103)) and agrees moderately with transpulmonary thermo-dye dilution techniques (104). Compared to other CBV optical methods (indicator dilution using radioisotopes or EB), it is the best (36,88,105,106). The Hb level should be measured from presampled blood before ICG injection to establish a baseline absorbance for the current patient, otherwise PDD accuracy is degraded significantly. CBV is calculated from a dilution curve of absorbance measured *in vivo* at the absorption maximum of ICG, and no subsequent blood sampling is necessary. The main drawback of PDD is its dependence on [Hb] measured *in vitro* prior the measurements which significantly increases the total CBV determination time (to hour scale). PDD also experiences several clinical problems: (*i*) in many liver diseases (e.g. cirrhosis (93)); (*ii*) PDD is irreproducible and much inaccurate for patients with low cardiac outputs, and PDD cannot entirely replace the pulmonary artery catheter (107); (*iii*) PDD cannot be used after surgery because of a low PDD signal amplitudes of optical detection of ICG (35); and (*iv*) further studies are needed to ascertain the impact of PDD on the mortality and morbidity of the critically ill patients (88).

Another method used in adults and infants weighing as little as 1000 g (108–112) is based on biotin labeling of either autologous or allogeneic RBCs with infusion back to bloodstream; CBV is determined by enumeration of labeled RBCs as a percentage of total RBCs in circulation measured with flow cytometry of a second blood sample. This method is accurate although it is relatively time-consuming and requires double blood sampling and knowledge of [Hb] for CBV calculation.

Thus, existing assays have provided a clinical justification and examples of utility of application of CBV measurement; however, no single method is feasible and reliable enough to be widely applied. Label dilution using radioisotopes or dyes are unsuitable for clinical application as they do not allow for frequent repeated measurements and require high concentrations of labeled proteins or contrast agents. The state-of-the-art method is PDD, and the use of ICG holds promise as the least invasive technique for measurement. However, the sensitivity and precision are not sufficient, and *a priori* data on Hb are required for each patient. Thus, currently there is no rapid (minutes scale), accurate (measurement error below 20%), low-cost and simple assay for CBV estimation with no *a priori* Hb information requirement.

Potential of PA/PT techniques

We emphasize here that PTFC, and especially PAFC technique (see above), after further development may likely offer advanced alternatives to existing methods. Indeed, PA imaging is currently the rapidly growing area of biomedical imaging, providing higher sensitivity and resolution in deeper tissues (up to 3 cm) compared to other optical modalities (113–117). PT method offers the highest absorption sensitivity (100–1000-fold better than PDD/optical absorption spectroscopy), which allows for noninvasive detection of unlabeled biomolecules at a threshold comparable with that of fluorescence labeling (118–121). The PA/PT methods are safe; the short-term temperature rise of ≤0.1–0.5°C at low laser fluence (5–20 mJ/cm^2) is well within the laser safety standard of 35–100 mJ/cm^2 at 650–1,100 nm (114). The tremendous clinical potential and safety of PA technique *in vivo* has been demonstrated in many clinical trials of other applications. Examples include imaging of breast tumors at depths of up to 3 cm (122–124) or blood microvessels (114), continuous monitoring of blood oxygenation in 15-mm-diameter jugular veins despite light scattering in a 15–20-mm-thick layer of overlying tissue, and measurement of blood [Hb] (124,125). However, the application of PA techniques for CBV measurement *in vivo* has not been reported. Such rapid PT/PA tests can be implemented as the determination of several dyes introduced in the blood as the difference in their absorption spectra can be used for the determination of their dilution without any additional information of blood parameter.

MATERIALS AND METHODS

The principle of *in vivo* photoacoustic flow cytometry with multicolor dyes

The principle of multispectral PAFC was described elsewhere (2–13). Briefly, in PAFC, objects of interest (e.g., cancer cells, nanoparticles, or dyes) in blood are irradiated by a focused laser beam (Fig. 1A). Laser-induced PA waves (referred to as PA signals) are detected with an ultrasound transducer attached to skin. The laser wavelengths are adjusted to absorption maximum of dyes. Figure 2 shows absorption spectra of several dyes that either are broadly used on preclinical animal models or were already approved for clinical use on humans (e.g., ICG) (79,126–131)). To prove the concept, we used available multicolor high-speed PAFC using lasers with high pulse rates. Dyes and laser wavelengths are selected to provide minimal overlapping between spectra bands of RBCs and dyes, in particular to achieve (*i*) the maximum PA contrast for RBCs (to measure [Hb] in the presence of dyes and (*ii*) the detection of dye at the lowest concentration (to minimize

possible toxicity) with reasonable (see below) accuracy and avoiding blood ([Hb]) interference (background). For example, for RBCs, MB and ICG, expected wavelengths should be around 530–570, 660–680, and 790–820 nm, respectively (Fig. 2). In particular, to detect a two-dye mixture (MB and ICG) we selected 671 nm and 820 nm.

The principle of measurements of circulating blood volume: phenomenological model

Three basic methods have been used to determine blood volume in humans using indicators (tags) (132,133). The first measures plasma volume using a plasma protein tag, the second measures the red cell volume by the injection of tagged RBCs and the third method depends on separate determinations of both plasma and RBC volume (true total volume determination). All the three methods are based on the dilution principle: agents are injected into the blood flow, dye dilution is monitored using spectrophotometry or other means (stated in the Introduction) and the dilution curve is recorded (Fig. 3). From this curve of the relative decrease in the dye concentration, CBV (V_{CBV}) is calculated from the ratio of dye concentrations of the initial solution and the diluted solution of dye in the blood according to the following simple equation (30,37,56,134):

$$V_{\mathrm{CBV}}=V_0\,A_x/A_0=V_0\,c_x/c_0, \quad (1)$$

Here, A is the signal amplitude, V_0 and c_0 are initial volume and concentration of the dye solution, and c_x is the equilibrium dye concentration in the blood after the dilution curve is developed, measured at equilibrium or calculated from multiple timed samples by extrapolation to zero time (Fig. 3). The volume of the agent injected can be neglected compared with the total volume of the blood (132). The precision of this approach is determined by the fact that mixing time is not significantly altered by either hypotension, shock, hypertension or congestive heart failure (135).

Total blood volume is calculated from the plasma or RBC volumes and a simultaneously determined Ht. For correct CBV assessment, three basic assumptions have to be met (132): (*i*) the indicator is tightly bound to the plasma protein or to the RBC used at least for the period of measurements; (*ii*) the plasma protein or tagged red all is uniformly mixed with the entire ‘plasma or volume’ to be determined, i.e., no important pools are sequestered away from the main intravascular space; and (*iii*) there is no loss of the indicator during the period of measurement or any loss occurs at a regular rate in order to allow back-calculation to time zero (132). These assumptions are better fulfilled by RBC tags than by plasma protein tags: there is virtually no loss of RBCs to the extravascular space in the short time needed for equilibration (132,133).

Calculation of total blood volume from either method assumes that Ht determined from peripheral blood samples is equal to the total body hematocrit; this was shown not to be the case (135,136). This difference, in part, is the result of the fact (the total blood volume calculated from red cell volume consistently underestimates (by 9–10%), but calculated from plasma volume consistently overestimates the true blood volume (by 5–10%) (49). To some extent, this can be accounted for by the use of correction factors based on the peripheral Ht. This precision is not always enough for correct clinical decisions. The method

depending on the determination of plasma and RBC volume is independent of Ht and therefore, provides a more accurate measure for total blood volume, although it takes much time as requires three independent tests, for Ht, for RBC-based measurements and for plasma-based measurements.

We propose to use two-dye mixtures for intravenous administration followed by dynamic PA/PT monitoring of their components in circulating blood. Thus, we propose to increase the number of dyes and the wavelengths for each dye and to use a more sensitive detection technique.

The use of a single wavelength is flawed as many spectral, spectrochemical and other factors affect the dilution curves. Thus, a single dye requires at least two wavelengths to improve precision (137,138). In blood, the introduction of wavelengths corresponding to Hb will allow the correction for blood absorption, which is used in PDD (35,78,79), however several wavelengths for Hb makes it possible to measure Hb species with increased precision.

Moreover in blood, we cannot use any wavelength of the dye; the selection depends on the interference with blood spectrum. Thus, the wavelength of a dye giving the maximum sensitivity could lie at a disadvantageous part of the spectrum (at steep growth/tailing parts, experiencing the interference from scattering, etc.) which would result in seriously degraded precision, which was discussed elsewhere (35,55,78,139). Thus, the use of a second dye, fully independent from the first with its own working wavelength pair considerably increases the precision of CBV assessment. Moreover, (*i*) if the maximum reproducibility is required, both dyes may be of the same type (RBC-bound or plasma-bound) or (*ii*) if we need the maximum accuracy (true CBV value), both dyes can be of different types; thus, we can estimate the true value of CBV in a single run. In fact, the dye cocktail could be comprised of three or more dyes, thus combining these two cases (*i*) and (*ii*).

Dye-cocktail techniques are extensively used in chemical analysis and *in vitro* tests, but this approach was not used in CBV measurements. This is not due to technical difficulties but because of the fact that simultaneous accurate determination of two (or more) dyes requires their significant concentrations, which is risky *in vivo*. The use of PA/PT techniques provide the increased precision over absorption measurements (140) at a concentration level at least 100-fold (usually more) lower.

As a whole, we approach the CBV assessment problem with (*i*) higher instrumental sensitivity; (*ii*) higher instrumental precision; (*iii*) lower toxicity of the measurements; and (*iv*) simultaneous implementation of all the CBV approaches and, thus, better assessment of true CBV.

Thus, the key idea is to intravenously inject two dyes with minimal overlap in absorption spectra with each other and with the absorption spectrum of the RBCs. Required concentrations are very low (submicromolar) and, hence nontoxic. Real-time PA monitoring of dye dilution and clearance at multiple wavelengths allows for a measurement of CBV because the dye concentration is inversely proportional to the ratio of CBV and injected dye volume. CBV (V_{CBV}) is measured as the average of two PA/PT signals for each dye to decrease the interference of both dyes and thus, to improve the accuracy. For two

simultaneously injected dyes, these calculations took into account the constraints $c_{0a} \approx c_{0b}$ and c_{0a}/c_{0b} = const, which are valid for pre-prepared dual mixtures of 'a' and 'b' dyes.

Direct assessment of c_x in Eq. (1) from PA/PT signals is needed in order to account for the effect of RBC absorption. Prior to these calculations, the signals are corrected using [Hb] determined from PA measurement at two wavelengths (e.g., 532 nm and 1064 nm) and background Hb absorption at selected wavelengths for the dyes. The determination of [Hb] is based on previously developed approach (141). In particular, we can measure the PT signals at 532 nm (or 610 nm, 635 nm, 660 nm and 690 nm, depending on the selected dye) and 1064 nm and calculate the total [Hb] at 532 nm and the fraction of HbO_2 at 1064 nm. An overdetermined Vierordt's equation system (*i*) at two wavelengths (142–146) is used for dyes and hemoglobin species at a nanomolar level (147).

$$\begin{cases} A^{\lambda_1} = l(c_a \varepsilon_a^{\lambda_1} + c_b \varepsilon_b^{\lambda_1}) \\ A^{\lambda_2} = l(c_a \varepsilon_a^{\lambda_2} + c_b \varepsilon_b^{\lambda_2}) \end{cases} . \quad (2)$$

and (*ii*) an overdetermined Vierordt's system at four wavelengths is used to further decrease the overall error (137,138):

$$\begin{cases} \Delta A_a = A^{\lambda_1} - A^{\lambda_2} = l[c_a(\varepsilon_a^{\lambda_1} - \varepsilon_a^{\lambda_2}) + c_b(\varepsilon_b^{\lambda_1} - \varepsilon_b^{\lambda_2})] \\ \Delta A_b = A^{\lambda_3} - A^{\lambda_4} = l[c_a(\varepsilon_a^{\lambda_3} - \varepsilon_a^{\lambda_4}) + c_b(\varepsilon_b^{\lambda_3} - \varepsilon_b^{\lambda_4})] \end{cases} . \quad (3)$$

Here *A* is absorbance acquired from PA measurements *in vivo* or calculated from PT measurements. As the wavelengths for Vierordt's method, the maxima of functions $\varepsilon_a^{\lambda_1}/\varepsilon_b^{\lambda_1}\sqrt{\varepsilon_a^{\lambda_1}\varepsilon_b^{\lambda_1}} = f(\lambda)$ and $\varepsilon_b^{\lambda_1}/\varepsilon_a^{\lambda_1}\sqrt{\varepsilon_a^{\lambda_1}\varepsilon_b^{\lambda_1}} = f(\lambda)$ are used. For the overdetermined system, Eq. (3), λ_1 and λ_3 are at the maxima, and λ_2 and λ_4 at the minima of the absorption spectra of 'a' and 'b' dyes.

Experimental setups

In vivo time-resolved PAFC setup was described elsewhere (8–13). Briefly, it was built on the platform of an Olympus BX51 microscope (Olympus America Inc.) and two pulsed lasers: (*i*) wavelength, 671 nm; pulse width, 25 ns; pulse rate, up to 100 kHz; pulse energy, 35 μJ (at 10 kHz rate); model, QL671-500, CrystaLaser, Reno, NV, USA; and (*ii*) wavelength, 820 nm; pulse width, 8 ns; pulse rate, up to 30 kHz; pulse energy, 70 μJ (at 10 kHz rate); model, LUCE 820, Bright Solutions. Laser radiation was delivered to the sample through microscope condenser.

PA signals from the transducer/amplifier (models XMS-310/5662; Panametrics) were recorded with a Tektronix TDS 3032B oscilloscope (Hayward, CA), or collected with a high-speed 200-MHz 12-bit ADC board (National Instruments, Austin, TX), LabVIEW software (National Instruments), and a Dell Precision 690 workstation.

To verify some *in vivo* PA data, *in vitro* PT measurements were performed with the setup described elsewhere (148). It is known that the basic physical effects are similar in PA and

PT methods, while the absorption sensitivity of PT spectrometry is better *in vitro* (149). Briefly, in continuous-wave (cw) mode PT thermal-lens schematic (Fig. 1B), is based on recording of laser-induced (lasers IDLS5, Polyus, Moscow; 532, 610, 635, 660, 690, 808, and 1064 nm; waist diameter, 80 ± 1 μm in sample; power range 20–50 mW) change of refractive index (thermal-lens effect) causing defocusing of a collinear diode laser probe beam (wavelength, 980 nm; waist diameter, 25.0 ± 0.2 μm; (attenuated) power, 0.4 mW). Hence a reduction in the probe beam intensity at its center (referred to as PT signal) is detected by a far-field (sample-to-detector distance 180 cm) photodiode with preamplifier (PDA36A, 40 dB amplification, ThorLabs Inc. with a 2-mm-diameter pinhole) as the response from a whole cell. (Fig. 1B). The synchronization of the measurements is implemented by in-house developed software. The PT spectrometer (148,150) has linear dynamic range of four orders of magnitude (the corresponding range of absorption coefficients for 10 mm optical pathway is 1×10^{-6} to 2×10^{-2} cm^{-1}) and response time of 0.005–2 s (depending on the selected measurement parameters, namely, data throughput rate and time, the number of points to be averaged, etc). The spectrometer implements a secondary channel for gathering scattered signal, if present. The probe beam is reflected by the dichroic mirror; the residual excitation beam is removed with a stained-glass bandpass filter and after a 2-mm pinhole appeared at the primary PT detector. If the photometric or PT channel is not needed, the corresponding detector is switched off. The scattering at the excitation wavelengths is collected with the secondary photodiode and used to correct the absorbance value, Eq. (6).

In this PT schematics, the advantages are (*i*) the possibility of detection under batch and flow conditions with no change in the optical-scheme design of the instrument; (*ii*) the possibility to switch between transient and steady-state thermal-lens measurements within a single set of experiments; and (*iii*) a wide linear dynamic range (see above).

Thermal-lens signal (148–150), θ, was acquired as a relative change in the probe-beam intensity at a far-field detector as traditionally used in PT spectroscopy (149) as

$$\theta = 2.303 P_e E \varepsilon l c = 2.303 P_e E A, \quad (4)$$

where P_e is the excitation laser power, E is the enhancement factor of PT lensing for unit excitation laser power (depends on geometry parameters of the optical scheme and thermal properties of the solution (149)), ε is the molar absorptivity, c is molar concentration of the dye in the sample, A is sample absorbance. For comparison, A from direct optical (photometric) measurements was compared with A recalculated from Eq. (4). The experimental values of the PT signal θ, were corrected to take into account the decrease in the excitation power due to light-scattering losses A_s in solutions:

$$q_{corr} = q(A + A_s)/A, \quad (5)$$

where A is sample absorbance. Whenever possible, the experimental values of sample absorbance, A_{exp}, were corrected for scattering effect

$$A = A_{exp} - A_s \quad (6)$$

Other measurements

Spectrophotometric measurements were made using a Shimadzu UV Mini 1240 spectrophotometer (Japan) with optical pathlength of 1 mm. The pH values were measured by an inoLab pH Level 1 pH-meter (Germany) with a glass pH-selective electrode (precision ±5%). Solutions were mixed with a Biosan MMS 3000 automixer. To model flow conditions *in vitro* with velocities in the range of 0.1–50 cm/s, we used a pump-driven system (KD Scientific Inc.) and glass tubes from 30 μm to 2 mm and a changeable vessel (volume 0.25 to 6 L). In most experiments, the flow rate was kept at 35 ± 1 mL/min (linear velocity 2 cm/s), a cylindrical flow cell (l = 15 mm; 16 cm^3) and tubings from a blood-transfusion system (KD Medical GmbH, Germany; length 90 cm, i.d. 0,3 cm) were used.

Reagents and solutions

The following dyes were used throughout: ICG, MB, BC, CV, IC (CAS no. 860-22-0), Bromsulphalein (CAS no. 71-67-0), and EB (Fig. 2) from Sigma-Aldrich (St. Louis, MO, USA). All the solutions were prepared in 0.10% wt. PBS (20 mM, pH 7.4). Water from a TW-600RU water purification system (Nomura MicroScience Co., Ltd.; Okada, Atsugi-City, Kanagawa, Japan) was used: pH 6.8; specific resistance 18.2 MΩ·cm, Fe, 2 ppt; dissolved SiO_2, 3 ppb; total ion amount, < 0.2 ppb; TOC, < 10 ppb. Solutions were made using a Branson 1510 ultrasonic bath (USA), power 1 W (exposure times 10 – 15 min). The blood of rats and mice stabilized with heparin was used at the stages of blood flow tests.

In Vitro Determination of Circulating Blood Volume by optical absorbance and photothermal spectroscopy—The main glass tube of the manifold was filled with the precisely measured blood volume, and the blood started circulating through the manifold. When the regular flow through the cuvette is established, the zero absorbance is calibrated. Next, 0.4 mL of a mixture of stock solutions of MB and CV was introduced, and the absorbances at 615, 630, 663 *и* 690 nm were recorded until constant absorbance/PT value values are reached (Fig. 3). The concentrations of both labels were determined from Eqs. (3).

Animal model

Nude mice (purchased from Harlan Sprague Dawley; weighing 20–25 g) were used in accordance with protocols approved by the University of Arkansas for Medical Sciences Institutional Animal Care and Use Committee. PA experiments were performed on the thin (~250 μm) mouse ear with well-distinguished blood vessels of 50 to 150 μm diameter at 50 to 100 μm depth. For *in vivo* monitoring of circulating dyes, mice were anesthetized with ketamine/xylazine, 50/10 mg/kg, I.p. The anesthetized mouse was placed on a temperature controlled microscope stage heated up to 37°C. The transducer was placed gently on the ear close to the laser beam. Topical application of warm water on the ear provided acoustic matching between the ultrasound transducer and the tissue. To adjust the laser beam in the vessel in PAFC, we used a 3D microstage with a back-synchronized algorithm (the

adjustment is made according to the maximum PA response from the object). We found that at the orientation of a linear beam shape across the vessel (perpendicular geometry), PA signals are less sensitive to the position of the laser beam on the skin, and hence, there is no strict need to control the position of the laser beam on vessels.

RESULTS

Spectrophotometric dye tests and CBV assessment *in vitro*

First, multiple dyes including MB, Brilliant Green, Crystal Violet, Congo Red, Indigo Carmine, Evans Blue, Bromsulphalein, and ICG were tested by conventional spectrophotometry in the presence and absence of blood to select the optimal clinically relevant dye, and wavelength providing minimal overlapping spectral effects, lowest concentration (i.e. with minimum possible toxicity but still enough for PT/PA detection), and required accuracy.

Absorption spectra of selected dyes (Fig. 2) do not significantly change in the pH range of 6.0–8.0 in the blood. As the aim was to develop a system for rapid analysis with low dye concentrations, we excluded IC, Bromsulphalein, and EB as the sensitivity of their spectrophotometric determination is low (151) and CBV assessment would require their high concentrations.

Spectrophotometric determination of MB, CV, ICG, and BG in aqueous solutions resulted in limits of detection of 1×10^{-7}M. Differential spectrophotometric determination of these label dyes against blood backgrounds of 0.5 – 2.0 absorbance units (compensated with the measurements at 532 and 1064 nm) showed a decrease in the sensitivity by an order, which can be considered satisfactory (Table) and correspond well to theoretical estimations of differential optical absorbance measurements (152,153).

As absorbance spectra of most dyes overlap (Fig. 2), Vierordt's method was used for data treatment. The comparison of variants of Vierordt's methods showed that the best results are obtained when the ratio of molar concentrations for both labels in a two-dye mixture is constant during all the tests. A two-wavelength Vierordt's system, Eq. (2), provides the error of 20% for micromolar concentrations of both dyes in a two-dye mixture. The use of the four-wavelength overdetermined system, Eq. (3), decreases the error to 7% (Fig. 4 and Table). In this case, the limits of detection of all the three dyes differ insignificantly from single dye solutions (Table).

The model flow manifold emulated a transfusion system: a 0.3 cm i.d., and the flow rate of 35 mL/min, the flow cell had the same diameter. The changes in the CBV within the range of 250 – 6000 mL showed that absorbance levels, reproducibility and accuracy of measurements for Hb and all the dyes do not depend on the volume. CV and MB showed negligible absorption on the materials of the transfusion system, while BG is intensively absorbed by the manifold. The flow spectrophotometric determination of individual labels in the transfusion manifold showed negligible difference from the batch conditions. For two-dye mixtures, the relative standard deviation of optical absorbance determination is below

10%, and is 2–5% for micromolar dye concentrations while using four-wavelength determination with an overdetermined Vierordt's system of equations (Fig. 4).

BG shows a very indistinct spectrum in the wavelength range of 600–650 nm in blood, while MB and CV show good differential spectra in 630–680 and 610–690 nm, respectively (Fig. 2). No correlation with their concentrations is obtained over 690 nm due to Hb absorption (Fig. 2). The optical absorbance limits of detection of all the three dyes in blood are at the level of 10^{-6} M (Table); and the error of determination is low, which makes it possible to determine CBV with two-dye mixtures with RSD below 10% at 10^{-5} M. With a spectrophotometer, varying the wavelengths of the Vierordt's systems, we selected the optimum wavelengths for the overdetermined system, 630 и 690 nm for MB and 610 and 660 nm for CV. For blood volumes 300 mL – 6 L, the error of measurements is below 4% (Fig. 4).

PT CBV assessment i*n vitro*

After the determination of performance parameters of CBV under the selected conditions with optical absorbance measurements, we shifted to PT spectroscopy, while retaining in *in vitro* area. The cw PT setup (Fig. 1B) sensitivity, time response, and accuracy of CBV measurements were evaluated *in vitro* under flow conditions (Table) to validate this platform for rapid, sensitive, and accurate CBV measurements with the advantages compared to existing assays. Working concentrations of all the used contrast agents were diminished by a factor of 50 compared to existing CBV methods to at least 10 nmol/l level (Table). This means the significant diminishing of dye doses to get reliable PT signals compared to current clinical doses (for PDD, 2.5–5 mg/mL ICG). From literature data, the linear absorption coefficient for ICG in blood is 43 cm^{-1} at 130 μM (0.1 mg/mL) while blood absorption at 808 nm is 4–5 cm^{-1} at 808 nm (154,155). The minimum delectable concentration of ICG in blood by PA/PT is 12 μM (0.01 mg/mL), which is 250 times lower than the clinically approved dose (155). The similar improvements are shown for other two dyes (Table).

Overall, from these experiments we may confidently predict that the advantage of *in vivo* PAFC measurements will be fast CBV assessment after (at least) a single dye injection. This allowed us to proceed to *in vivo* PAFC tests.

In vivo PA monitoring of clearance rate of dye cocktail

Finally, we estimated the capability of PAFC to in vivo simultaneously monitor two intravenously injected dyes. We selected dual mixture of ICG and MB with almost non-overlapped absorption spectra (Fig. 2). Intravenous injection of this dye cocktail (ICG, 70 μl; MB, 15 μl, both 5 mg/ml) into a mouse circulatory system through the tail vein was followed by dye clearance monitoring from vessels in ear using the PAFC. In this study, we used a high pulse repetition rate lasers (both 10 kHz) with wavelengths of 671 nm and 820 nm, which lie in spectral range near the maximum absorption of MB and ICG, respectively (Fig. 2). The PA signals from ear blood vessels before dye injection 2–4-fold higher than the PA background signals from the surrounding tissue. The continuous monitoring of PA signals from these vessels after injections revealed fast (from few to dozens seconds) dye

appearance in blood flow which is followed by its clearance (Fig. 5). The average clearance time of ICG and MB was found in the range of 5–10 min, which is in very good consistence with *in vitro* PT tests and other published data (5). During this study we observed often strong PA signals immediately (within few seconds) after dye injection (not shown) that are likely associated with the initial peak of the dilution curve (Fig. 3). However, these PA signals were not stable with significant amplitude fluctuation. We explain these phenomena by the limitation of both animal modesl used with fast (seconds scale) averaging of dye in small blood mouse volume (~2 mL), and not immediate tail injection procedure lasted for trained personal at least (1–3 seconds).

We observed also strong fluctuated PA signals above the continuous background signals from both ICG and MB started approximately after 1 to 3 minutes after injection. We could not avoid these phenomena even after careful cleaning, centrifuging, and filtering of the dyes, verified by no sign of visible aggregates with high-resolution transmission microscopy. Hypothetically, the origin of these flashed PA signals may be related with difficult to control phenomena associated with increased local dye concentration. It could be either nanoscale dye aggregates in the initial solution not detectable with diffraction-limited optical microscope, aggregation of dye molecule itself in blood flow, interaction of dye molecules with plasma proteins, accumulation of slow moving dye molecules near vessel walls, and adherence (or uptake) of dyes on endothelial cells leading to dye overheating accompanied by random bubble formation, or dye uptake by some blood cells. The widths of the most flash PA signals were in the range of 3–5 ms. Considering the linear laser beam width of 10 μm, and expected flow velocity of 3–7 mm/s, flash PA signal widths correspond to the target size of approximately 9–20 μm, which is comparable to blood cell sizes. Comparison of PA signal traces at different signal averaging (Fig. 5, A and B) revealed a decrease in the signal amplitude with increased averaging. This finding suggests that the signals are coming from small targets which provide a limited number (20–50) of PA flashes during crossing the laser beam. As a result, averaging at longer time than lifetime of flowing objects in the detected volume led to decrease in detection sensitivity of sharp PA signals, although background noise becomes lower. Thus, the observed PA signal fluctuations can be associated, at least at longer time after injection, with the ability of some blood cells, in particular reticulocytes and leukocytes, to significantly uptake ICG and MB, respectively, directly in blood flow leading to increased local dye concentration within these cells (155–157).

For TB, we observed smaller number of PA peaks with lower amplitudes, compared to ICG and MB (Fig. 6). TB is broadly used for cell viability tests due to its effective uptake by dead cells (158,159). If it takes place *in vivo* in our experiments, number of circulating dead cells should be much smaller compared to normal blood cells, due to their fast clearance by the reticuloendothelial system. This is in agreement with obtained data (Fig. 6).

Besides, the wavelength used (671 nm) is outside the strong absorption band of Trypan Blue, which can explain smaller PA signal amplitudes from Trypan Blue compared to ICG or MB.

To verify the capability of PAFC to detect in vivo individual circulating cells with high local dye concentration we extracted small amount of blood from mice, separated RBCs, and WBCs according to standard procedures, and incubated these cells with ICG and MB at different conditions (RBCs with 150 μg/ml ICG were incubated for 60 min at 37°C. WBCs with 850 μg/ml MB were incubated for 30 min at 37°C). We found found significant (5–30 times) increase PT signals from labeled cells compared to control cells. Cells were injected back intravenously to mouse circulation in concentration approximately 10^5 RBCs and 10^4 WBCs. Monitoring of ear blood microvessels with two color PAFC (671/820 nm) revealed PA signal traces at both wavelengths (Fig. 7) associated with circulated labeled RBCs and WBCs.

This funding suggests possibility of labeling of RBCs and WBCs with conventional dyes, the capability of PAFC to detect circulating cells labeled with these dyes, and potential to use this approach for measurement of CBV.

DISCUSSION

Thus, we successfully demonstrated the feasibility of PP for blood volume measurements. We also showed the capability of two-color PAFC to monitor simultaneously two dyes (ICG and MB) in blood circulation as well as to detect circulating blood cells labeled with these dyes. These studies establish a platform which could be used further for in vivo PA blood volume measurements. From our data, we estimate the absolute limit of detection for ICG to be 2 fmol in a 60×60×60 μm probed blood volume (in a vessel). Also, we confirmed that the implementation of the 4-wavelength system in PT measurements generated an error of <7% for nanomolar concentrations of both dyes in a blood flow (Fig. 4). The measurement provided a decrease in the contrast agent concentrations by a factor of at least 30 due to the high absorption sensitivity of PT/PA spectroscopy and low influence of scattering effects (149). Moreover, we showed a decrease in the error of measurements by a factor of 3–4 compared to existing CBV techniques due to the independent determination of two dyes instead of one at two different wavelengths (Fig. 4). The determination of [Hb] simultaneously with dye dilution provided lower measurement time (2–4 fold) compared to photometric CBV techniques and PDD (148). Labeling of extracted RBCs with clinically approved dyes (e.g., ICG) and infusing them back to bloodstream open door for new methods of CBV measurements by enumeration of labeled RBCs as a per cent of total RBCs in circulation measured with PAFC in vivo.

The ability of PA and PT techniques to detect conventional agents was related to their limited quantum yield, typically in the range of 1–20%, resulting in transformations of most absorbed energy into heat, to which the PT/PA technique is very sensitive (149). The most PA imaging algorithms currently in use for signal acquisition are not quite suitable for rapid real-time PA monitoring of contrast agent dynamics in the fast blood flow due to their time-consuming signal acquisition process. As described here, the time-resolved PAFC mode with good temporal resolution (0.1–1 ms) allowed us to observe strong dynamic fluctuation of PA signals from dyes in bloodstream (Fig. 6). This phenomenon can be explained by either high sensitivity of PAFC to small nano- and micro-dye aggregates in blood flow or strong uptake of dyes by blood cells, in (155–157). As a result, this labeling directly in blood

flow (*in vivo* cell staining) can be used for detection and counting of these cells using multicolor PAFC. We cannot also exclude dye uptake by circulating dead cells. A control experiment with Trypan Blue, which is broadly used for viability tests *in vitro*, revealed rare notable PA signals *in vivo* which can be associated with rare dead cells with extremely high clearance rate (Fig. 7). Thus, in addition to previously demonstrated detection of circulating normal and apoptotic cells we show here potential to use of PAFC for detection of circulating dead cells. This is important for many applications including studies of cell metabolism in norm and pathological states or response to various therapies (Fig. 8). However, these and similar effects require future detailed studies, and PAFC is the ideal tool for dynamic study of cell-dye interaction *in vivo*. These fluctuations are not important from the point of view of measurement of circulation time or CBV, since the increased averaging of PA signals (Fig. 5B) easily minimizes the influence of these effects.

In general, we showed the possibilities of our platform for optical absorption, PT, and PA determination of two dyes in a transfusion system. The expected precision of measurements is better than in pulse dye densitometry (35,78,79), but for concentrations two orders lower (down to nanomolar concentrations and femtomolar amounts of dyes (49,50,55,56). Our platform does not require any *a priori* data on the blood parameters, and is very robust.

The use of high pulse repetition rate lasers (10–100 kHz) provided significant averaging of the signal and a 100-fold increase in the detection sensitivity (as square root of pulse rate ratio). This provides a significant decrease in the laser pulse energy, thus offering better safety of the patients while retaining enough sensitivity to reliably measure multi-component dye cocktails at their low, non-hazardous concentrations.

After further improvement of this technology, we anticipate that the noninvasive, rapid, real-time measurement of CBV will be a valuable tool for monitoring surgical patients in the operating room, especially those undergoing surgery with predictable substantial blood loss. The high capacity of this advanced multicolor PAFC technique will provide measurement of CBV with expected advantages in accuracy, time response, and sensitivity compared to existing assays. Successful completion of these specific aims will provide a novel method for CBV measurements *in vivo* and will shift clinical paradigms by achieving unprecedented high sensitivity (50–100-fold higher than existing techniques), rapid turnaround (a few minutes *vs.* hour-scale due to exclusion of any *a priori* information on the patient) and high accuracy (5–7% *vs.* 15–30%). This method also offers several long-term spinoffs. The proposed platform can be further applied to PA measurement of multiple blood parameters including a total Hb amount, Ht, oxygenation, abnormal blood cells (e.g., sickle), and Hb composition (e.g., meta-, carboxy-, nitroso- or HbS [e.g., in sickle cells]) during various diseases (e.g., anemia) as well as on use of encapsulated dyes (106,107,129–137). Changes of ICG clearance rate can also be used for diagnosis of liver dysfunction. We plan a preclinical validation with a larger animal model (e.g., rabbit or sheep) and eventually clinical trials using finger, nose, lip, and hand vessels.

The clinical prototype could be developed as a portable device with two diode lasers and small ultrasound transducer (Fig. 8) that overlies the different vessels, ranging from capillaries in the nailfold to large vessels in the neck area.

Spectral specificity of multicolor PAFC may be limited by relatively broad absorption bands of dyes and their overlapping when dyes were injected together. This problem can be overcome by using high resolution nonlinear PT and PA spectroscopy (13). It demonstrated narrowing of absorption spectra of dyes near absorption maximum that can be used for multicolor PAFC.

Acknowledgments

This work was supported in part by the National Institute of Health, grant numbers R01CA131164, R01 EB009230, and R21CA139373, the National Science Foundation, grant numbers DBI-0852737, and Department of Defense grants: W88XWH-10-2-0130, W81XWH-10-BCRP-CA, and W81XWH-11-1-0129 and in part by the Russian Foundation for Basic Research, grants nos. 10-02-01354-a and 10-03-01018-a and the Ministry of Science and Technology of Russian Federation, contract no. 16.740.11.0471. We would like to thank Dmitry Nedosekin and Scott Fergusson for their help in laser experiments and Jian-Hui Ye for sample preparation.

References

1. Shapiro, HM. Practical Flow Cytometry. New York: Wiley-Liss; 2003.
2. Zharov, VP.; Galanzha, EI.; Tuchin, VV. Photothermal imaging of moving cells in lymph and blood flow in vivo. Oraevsky, AA.; Wang, LV., editors. San Jose, CA, USA: SPIE; 2004. p. 185-195.
3. Zharov VP, Galanzha EI, Tuchin VV. Photothermal image flow cytometry in vivo. Opt Lett. 2005; 30:628–630. [PubMed: 15791998]
4. Zharov VP, Galanzha EI, Tuchin VV. In vivo photothermal flow cytometry: Imaging and detection of individual cells in blood and lymph flow. J Cell Biochem. 2006; 97:916–932. [PubMed: 16408292]
5. Zharov VP, Galanzha EI, Shashkov EV, Khlebtsov NG, Tuchin VV. In vivo photoacoustic flow cytometry for monitoring of circulating single cancer cells and contrast agents. Opt Lett. 2006; 31:3623–3625. [PubMed: 17130924]
6. Zharov VP, Galanzha EI, Shashkov EV, Kim JW, Khlebtsov NG, Tuchin VV. Photoacoustic flow cytometry: principle and application for real-time detection of circulating single nanoparticles, pathogens, and contrast dyes in vivo. J Biomed Opt. 2007:12.
7. Galanzha EI, Shashkov EV, Tuchin VV, Zharov VP. In vivo multispectral, multiparameter, photoacoustic lymph flow cytometry with natural cell focusing, label-free detection and multicolor nanoparticle probes. Cytometry Part A. 2008; 73A:884–894.
8. Galanzha EI, Shashkov EV, Spring PM, Suen JY, Zharov VP. In vivo, Noninvasive, Label-Free Detection and Eradication of Circulating Metastatic Melanoma Cells Using Two-Color Photoacoustic Flow Cytometry with a Diode Laser. Cancer Res. 2009; 69:7926–7934. [PubMed: 19826056]
9. Galanzha EI, Kim JW, Zharov VP. Nanotechnology-based molecular photoacoustic and photothermal flow cytometry platform for in-vivo detection and killing of circulating cancer stem cells. J Biophotonics. 2009; 2:725–35. [PubMed: 19957272]
10. Nedosekin DA, Sarimollaoglu M, Shashkov EV, Galanzha EI, Zharov VP. Ultra-fast photoacoustic flow cytometry with a 0.5 MHz pulse repetition rate nanosecond laser. Opt Express. 2010; 18:8605–20. [PubMed: 20588705]
11. Galanzha EI, Shashkov EV, Kelly T, Kim JW, Yang L, Zharov VP. In vivo magnetic enrichment and multiplex photoacoustic detection of circulating tumour cells. Nat Nanotechnol. 2009; 4:855–60. [PubMed: 19915570]
12. Kim JW, Galanzha EI, Shashkov EV, Moon HM, Zharov VP. Golden carbon nanotubes as multimodal photoacoustic and photothermal high-contrast molecular agents. Nat Nanotechnol. 2009; 4:688–694. [PubMed: 19809462]
13. Zharov VP. Ultrasharp nonlinear photothermal and photoacoustic resonances and holes beyond the spectral limit. Nat Photon. 2011; 5:110–116.

14. Biris AS, Galanzha EI, Li ZR, Mahmood M, Xu Y, Zharov VP. In vivo Raman flow cytometry for real-time detection of carbon nanotube kinetics in lymph, blood, and tissues. J Biomed Opt. 2009:14.
15. Shashkov EV, Galanzha EI, Zharov VP. Photothermal and photoacoustic Raman cytometry in vitro and in vivo. Opt Express. 2010; 18:6929–6944. [PubMed: 20389713]
16. Tuchin VV. Laser light scattering in biomedical diagnostics and therapy. J Laser Appl. 1993; 5:43–60. [PubMed: 10146408]
17. Novak J, Georgakoudi I, Wei X, Prossin A, Lin CP. In vivo flow cytometer for real-time detection and quantification of circulating cells. Opt Lett. 2004; 29:77–9. [PubMed: 14719666]
18. Georgakoudi I, Solban N, Novak J, Rice WL, Wei X, Hasan T, Lin CP. In vivo flow cytometry: a new method for enumerating circulating cancer cells. Cancer Res. 2004; 64:5044–7. [PubMed: 15289300]
19. Wei X, Sipkins DA, Pitsillides CM, Novak J, Georgakoudi I, Lin CP. Real-time detection of circulating apoptotic cells by in vivo flow cytometry. Mol Imaging. 2005; 4:415–6. [PubMed: 16285902]
20. Boutrus S, Greiner C, Hwu D, Chan M, Kuperwasser C, Lin CP, Georgakoudi I. Portable two-color in vivo flow cytometer for real-time detection of fluorescently-labeled circulating cells. J Biomed Opt. 2007; 12:020507. [PubMed: 17477705]
21. He W, Wang H, Hartmann LC, Cheng JX, Low PS. In vivo quantitation of rare circulating tumor cells by multiphoton intravital flow cytometry. Proc Natl Acad Sci U S A. 2007; 104:11760–5. [PubMed: 17601776]
22. Tkaczyk ER, Zhong CF, Ye JY, Myc A, Thomas T, Cao Z, Duran-Struuck R, Luker KE, Luker GD, Norris TB, et al. In Vivo Monitoring of Multiple Circulating Cell Populations Using Two-photon Flow Cytometry. Opt Commun. 2008; 281:888–894. [PubMed: 19221581]
23. Zhong CF, Tkaczyk ER, Thomas T, Ye JY, Myc A, Bielinska AU, Cao Z, Majoros I, Keszler B, Baker JR, et al. Quantitative two-photon flow cytometry--in vitro and in vivo. J Biomed Opt. 2008; 13:034008. [PubMed: 18601553]
24. Chang YC, Ye JY, Thomas TP, Cao Z, Kotlyar A, Tkaczyk ER, Baker JR Jr, Norris TB. Fiber-optic multiphoton flow cytometry in whole blood and in vivo. J Biomed Opt. 2010; 15:047004. [PubMed: 20799835]
25. de la Zerda A, Kim J-W, Galanzha EI, Gambhir SS, Zharov VP. Advanced contrast nanoagents for photoacoustic molecular imaging, cytometry, blood test, and phototohermal theranostics. Contrast Media and Molecular Imaging. 2011 in press.
26. Nedosekin DA, Sarimollaoglu M, Shashkov EV, Galanzha EI, Zharov VP. Ultra-fast photoacoustic flow cytometry with a 0.5 MHz pulse repetition rate nanosecond laser. Opt Express. 2010; 18:8605–8620. [PubMed: 20588705]
27. Galanzha EI, Tuchin VV, Zharov VP. In vivo integrated flow image cytometry and lymph/blood vessels dynamic microscopy. J Biomed Opt. 2005:10.
28. Tanev S, Sun W, Pond J, Tuchin VV, Zharov VP. Flow cytometry with gold nanoparticles and their clusters as scattering contrast agents: FDTD simulation of light-cell interaction. J Biophotonics. 2009; 2:505–20. [PubMed: 19670359]
29. Roche-Labarbe N, Carp SA, Surova A, Patel M, Boas DA, Grant PE, Franceschini MA. Noninvasive optical measures of CBV, StO(2), CBF index, and rCMRO(2) in human premature neonates' brains in the first six weeks of life. Hum Brain Mapp. 2010; 31:341–52. [PubMed: 19650140]
30. Takanishi DM Jr, Biuk-Aghai EN, Yu M, Lurie F, Yamauchi H, Ho HC, Chapital AD, Koss W. The availability of circulating blood volume values alters fluid management in critically ill surgical patients. Am J Surg. 2009; 197:232–7. [PubMed: 19185111]
31. Jahr JS, Lurie F, Bezdikian V, Driessen B, Gunther RA. Measuring circulating blood volume using infused hemoglobin-based oxygen carrier (oxyglobin) as an indicator: verification in a canine hypovolemia model. Am J Ther. 2008; 15:98–101. [PubMed: 18356627]
32. Aladangady N, Leung T, Costeloe K, Delpy D. Measuring circulating blood volume in newborn infants using pulse dye densitometry and indocyanine green. Paediatr Anaesth. 2008; 18:865–71. [PubMed: 18544143]

33. Kuntscher MV, Germann G, Hartmann B. Correlations between cardiac output, stroke volume, central venous pressure, intra-abdominal pressure and total circulating blood volume in resuscitation of major burns. Resuscitation. 2006; 70:37–43. [PubMed: 16759783]
34. Lozhkin A, Makedonskaya T, Pakhomova G, Loran O. Estimation of the Trauma Severity Degree in Injured with Associated Injuries Depending on the Blood Loss. Vox Sanguinis. 2010; 99:435–436.
35. Baulig W, Bernhard EO, Bettex D, Schmidlin D, Schmid ER. Cardiac output measurement by pulse dye densitometry in cardiac surgery. Anaesthesia. 2005; 60:968–73. [PubMed: 16179040]
36. Kroon M, Groeneveld AB, Smulders YM. Cardiac output measurement by pulse dye densitometry: comparison with pulmonary artery thermodilution in post-cardiac surgery patients. J Clin Monit Comput. 2005; 19:395–9. [PubMed: 16437290]
37. Henschen S, Busse MW, Zisowsky S, Panning B. Determination of plasma volume and total blood volume using indocyanine green: a short review. J Med. 1993; 24:10–27. [PubMed: 8501401]
38. Donner L, Maly V. Total blood volume in some blood diseases. II. Results in pernicious anemia, anemia following hemorrhage, polycythemia vera, secondary polyglobulia and leukemia. Sb Lek. 1955; 57:125–36. [PubMed: 14396265]
39. Tanaka K, Sato T, Kondo C, Yada I, Yuasa H, Kusagawa M, Nasu M, Okada Y, Shomura T. Hematological problems during the use of cardiac assist devices: clinical experiences in Japan. Artif Organs. 1992; 16:182–8. [PubMed: 10078242]
40. Schleyer F. Photometric determination of the amounts of dried-up traces of blood, from their hemoglobin content, determined as cyanic hemiglobin. Blut. 1968; 17:20–4. [PubMed: 5689469]
41. Giubileo M, Grisler R. Quantitative analysis of total hemoglobin pigments in blood; comparision of two photometric methods. Med Lav. 1959; 50:301–6. [PubMed: 13673773]
42. Spett K. Photometric method for the determination of oxyhemoglobin/total hemoglobin ratio in blood. Acta Biochim Pol. 1957; 4:117–28. [PubMed: 13468986]
43. Harzheim J, Kunzer W, Savelsberg W. Blood bilirubin level and photometric hemoglobin determination. Klin Wochenschr. 1951; 29:95. [PubMed: 14825770]
44. Soprunov FF, AKh B. Gravimetric method for the determination of the specific gravity of blood, plasma proteins, hemoglobin content and hematocrit values. Vopr Med Khim. 1956; 2:452–6. [PubMed: 13423131]
45. Orsini JJ, Yeman J, Caggana M, Bodamer OA, Muhl A. Semi-quantitative method for determination of hematocrit in dried blood spots, using data collected in HPLC hemoglobin variant testing. Clin Chim Acta. 2010; 411:894–5. [PubMed: 20230811]
46. Shul'man KM, Shitikova MG. A comparative assessment of the isotope (Cr51), gravimetric and clinical methods of observation of the volume of circulating blood in extracorporeal circulation. Med Radiol (Mosk). 1966; 11:57–62. [PubMed: 5989749]
47. Keith NM, Rowntree LG, Geraghty JT. Method for the determination of plasma and blood volume. Archives of Internal Medicine. 1915; 16:547–557.
48. Jegier W, Maclaurin J, Blankenship W, Lind J. Comparative Study of Blood Volume Estimation in the Newborn Infant Using I-131 Labeled Human Serum Albumin (Ihsa) and T-1824. Scand J Clin Lab Invest. 1964; 16:125–32. [PubMed: 14161845]
49. Uglova NN, Volozhin AI, Potkin VE. Method for determination of the circulating blood volume with Evans blue T-1824. Patol Fiziol Eksp Ter. 1972; 16:80–2. [PubMed: 5044400]
50. Glants SA, Shevchuk VV. A Micromethod for the Determination of Blood Volume in Laboratory Animals. Lab Delo. 1963; 16:49. [PubMed: 14064268]
51. Gillen CM, Takamata A, Mack GW, Nadel ER. Measurement of plasma volume in rats with use of fluorescent-labeled albumin molecules. J Appl Physiol. 1994; 76:485–9. [PubMed: 8175546]
52. Tudhope GR, Wilson GM. A comparison of 86Rb, 32P and 51Cr as labels for red blood cells. J Physiol. 1955; 128:61–2P. [PubMed: 13243356]
53. Sivachenko TP, Kalina VK, Ishchenko VP, Belous AK, Kapustnik VI. Repeated semi-automatic determination of circulating blood volume. Vrach Delo. 1977:25–8. [PubMed: 898862]
54. Gray SJ, Sterling K. Determination of circulating red cell volume by radioactive chromium. Science. 1950; 112:179–80. [PubMed: 15442294]

55. Datsenko BM, Pilipenko NI, Gubskii VI, Sherlanov RA. The determination of the volume of circulating plasma using the indicator T-1824. Lab Delo. 1990:32–4. [PubMed: 1704951]
56. Kovalev OA, Grishanov VN. Determination of the volume of circulating blood by using Evans blue dye. Lab Delo. 1976:664–7. [PubMed: 66351]
57. Gibson JG, Seligman AM, Peacock WC, Aub JC, Fine J, Evans RD. The Distribution of Red Cells and Plasma in Large and Minute Vessels of the Normal Dog, Determined by Radioactive Isotopes of Iron and Iodine. J Clin Invest. 1946; 25:848–57.
58. Modestov VK, Tsygankov AT. Thyroid Function Tests Using Triiodothyronine Labelled with I-131. Med Radiol (Mosk). 1965; 10:11–3. [PubMed: 14340477]
59. Frid IA, Stoliarov VI, Evtiukhin AI, Bernshtein MI. Hemodynamic indices and the volume of circulating blood in the surgical treatment of cancer of the esophagus and cardial portion of the stomach. Vestn Khir Im I I Grek. 1976; 117:92–6. [PubMed: 1014238]
60. Kirkin BV, Rumiantsev VG, Kabanova IN. Evaluation of blood loss volume and the degree of activity of nonspecific ulcerative colitis by using Cr51-labeled erythrocytes. Khirurgiia (Mosk). 1990:57–61. [PubMed: 2359244]
61. Lomakin MM, Geishtovt GM. Donor blood erythrocyte tag with Cr51 for determination of circulating blood volume. Med Radiol (Mosk). 1972; 17:38–9. [PubMed: 4662734]
62. Wels A, Schnappauf H, Horn V. Blood volume determinations in fowls with Cr51 and T- 1824. Zentralbl Veterinarmed A. 1967; 14:741–6. [PubMed: 4970164]
63. Klement AW Jr, Ayer DE, Rogers EB. Simultaneous use of Cr51 and T-1824 dye in blood volume studies in the goat. Am J Physiol. 1955; 181:15–8. [PubMed: 14376560]
64. Klement AW Jr, Ayer DE, Mc ID. Simultaneous use of I131-albumin and Cr51-labelled red cells in blood volume studies in the goat. Proc Soc Exp Biol Med. 1954; 87:81–5. [PubMed: 13224684]
65. Burger T, Keszthelyi B, Peer J. Pathological significance of blood volume changes in untreated polycythemia vera and after P32 therapy. Pathol Biol (Paris). 1962; 103:357–60. [PubMed: 13874809]
66. Basu B, Bhattacherjee KL, Bose A. Comparative estimation of blood volume by P32 tagged red cells and dye haematocrit method in human subjects. J Indian Med Assoc. 1957; 28:469–72. [PubMed: 13449332]
67. Gamble JL Jr, Klement AW Jr, Rogers EB. Scintillation counter assay of I131 and P32 in blood volume studies. Proc Soc Exp Biol Med. 1954; 85:172–4. [PubMed: 13134326]
68. Bohr H. Blood volume determination by P32-labelled blood cells. Ugeskr Laeger. 1952; 114:1522–5. [PubMed: 13029248]
69. Berson SA, Yalow RS, Azulay A, Schreiber S, Bernard R, Roswit B. The biological decay curve of P32 tagged erythrocytes; application to the study of acute changes in blood volume. J Clin Invest. 1952; 31:581–91. [PubMed: 14938437]
70. Berson SA, Yalow RS. The use of K42 or P32 labeled erythrocytes and I131 tagged human serum albumin in simultaneous blood volume determinations. J Clin Invest. 1952; 31:572–80. [PubMed: 14938436]
71. Brown FA Jr, Hempelmann LH Jr, Elman R. The Determination of Blood Volume with Red Blood Cells Containing Radioactive Phosphorus (P32). Science. 1942; 96:323–4. [PubMed: 17751372]
72. Hayakawa J, Tsuchiya T, Eto H. The effects of spleen shielded irradiation on 59Fe incorporation into red blood cells in three different strains of mice. Nippon Igaku Hoshasen Gakkai Zasshi. 1968; 27:1425–9. [PubMed: 5244663]
73. Thunell S. Determination of Incorporation of 59fe in Hemin of Peripheral Red Blood Cells and of Red Cells in Bone Marrow Cultures. Clin Chim Acta. 1965; 11:321–33. [PubMed: 14323677]
74. de FJ, da GA. Determination by radioactive iron (59Fe) of the amount of blood ingested by insects. Bull World Health Organ. 1961; 25:271–3. [PubMed: 13895001]
75. Soprunov FF, Stefanovskaia NV, Kurbanov K. The rate of turnover and the nature of biosynthesis of proteins in the blood plasma and skin in the rabbit. Vopr Med Khim. 1965; 11:46–54. [PubMed: 5885695]
76. Leipala JA, Talme M, Viitala J, Turpeinen U, Fellman V. Blood volume assessment with hemoglobin subtype analysis in preterm infants. Biol Neonate. 2003; 84:41–4. [PubMed: 12890935]

77. Margarson MP, Soni NC. Plasma volume measurement in septic patients using an albumin dilution technique: comparison with the standard radio-labelled albumin method. Intensive Care Med. 2005; 31:289–95. [PubMed: 15526187]

78. Haruna M, Kumon K, Yahagi N, Watanabe Y, Ishida Y, Kobayashi N, Aoyagi T. Blood volume measurement at the bedside using ICG pulse spectrophotometry. Anesthesiology. 1998; 89:1322–8. [PubMed: 9856705]

79. Imai T, Takahashi K, Fukura H, Morishita Y. Measurement of cardiac output by pulse dye densitometry using indocyanine green: a comparison with the thermodilution method. Anesthesiology. 1997; 87:816–22. [PubMed: 9357883]

80. Ishikawa M, Nishioka M, Hanaki N, Kikutsuji T, Miyauchi T, Kashiwagi Y, Miki H. Postoperative metabolic and circulatory responses in patients that express SIRS after major digestive surgery. Hepatogastroenterology. 2006; 53:228–33. [PubMed: 16608030]

81. Sugimoto H, Okochi O, Hirota M, Kanazumi N, Nomoto S, Inoue S, Takeda S, Nakao A. Early detection of liver failure after hepatectomy by indocyanine green elimination rate measured by pulse dye-densitometry. J Hepatobiliary Pancreat Surg. 2006; 13:543–8. [PubMed: 17139429]

82. Hori T, Yagi S, Iida T, Taniguchi K, Yamagiwa K, Yamamoto C, Hasegawa T, Yamakado K, Kato T, Saito K, et al. Stability of cirrhotic systemic hemodynamics ensures sufficient splanchnic blood flow after living-donor liver transplantation in adult recipients with liver cirrhosis. World J Gastroenterol. 2007; 13:5918–25. [PubMed: 17990357]

83. Hoff RG, van Dijk GW, Algra A, Kalkman CJ, Rinkel GJ. Fluid balance and blood volume measurement after aneurysmal subarachnoid hemorrhage. Neurocrit Care. 2008; 8:391–7. [PubMed: 18172784]

84. Ishikawa M, Nishioka M, Hanaki N, Miyauchi T, Kashiwagi Y, Kawasaki Y, Miki H, Kagawa H, Ioki H, Nakamura Y. Postoperative host responses in elderly patients after gastrointestinal surgery. Hepatogastroenterology. 2006; 53:730–5. [PubMed: 17086878]

85. Sha K, Shimokawa M, Morii M, Kikumoto K, Inoue S, Kishi K, Kitaguchi K, Furuya H. Optimal dose of indocyanine-green injected from the peripheral vein in cardiac output measurement by pulse dye-densitometry. Masui. 2000; 49:172–6. [PubMed: 10707522]

86. Taguchi N, Nakagawa S, Miyasaka K, Fuse M, Aoyagi T. Cardiac output measurement by pulse dye densitometry using three wavelengths. Pediatr Crit Care Med. 2004; 5:343–50. [PubMed: 15215003]

87. Fujita Y, Yamamoto T, Fuse M, Kobayashi N, Takeda S, Aoyagi T. Pulse dye densitometry using indigo carmine is useful for cardiac output measurement, but not for circulating blood volume measurement. Eur J Anaesthesiol. 2004; 21:632–7. [PubMed: 15473618]

88. Goy RW, Chiu JW, Loo CC. Pulse dye densitometry: a novel bedside monitor of circulating blood volume. Ann Acad Med Singapore. 2001; 30:192–8. [PubMed: 11379418]

89. Imai T, Mitaka C, Nosaka T, Koike A, Ohki S, Isa Y, Kunimoto F. Accuracy and repeatability of blood volume measurement by pulse dye densitometry compared to the conventional method using 51Cr-labeled red blood cells. Intensive Care Med. 2000; 26:1343–9. [PubMed: 11089762]

90. Kunihara T, Wakamatsu Y, Adachi A, Koyama M, Shiiya N, Sasaki S, Murashita T, Matsui Y, Yasuda K. Clinical evaluation of hepatic blood flow and oxygen metabolism during thoracoabdominal aortic surgery using pulse dye-densitometry combined with hepatic venous oxygen saturation. Kyobu Geka. 2000; 53:551–7. [PubMed: 10897566]

91. Mizushima Y, Tohira H, Mizobata Y, Matsuoka T, Yokota J. Assessment of effective hepatic blood flow in critically ill patients by noninvasive pulse dye-densitometry. Surg Today. 2003; 33:101–5. [PubMed: 12616369]

92. Akita H, Sasaki Y, Yamada T, Gotoh K, Ohigashi H, Eguchi H, Yano M, Ishikawa O, Imaoka S. Real-time intraoperative assessment of residual liver functional reserve using pulse dye densitometry. World J Surg. 2008; 32:2668–74. [PubMed: 18841411]

93. Stauber RE, Wagner D, Stadlbauer V, Palma S, Gurakuqi G, Kniepeiss D, Iberer F, Smolle KH, Haas J, Trauner M. Evaluation of indocyanine green clearance and model for end-stage liver disease for estimation of short-term prognosis in decompensated cirrhosis. Liver Int. 2009; 29:1516–20. [PubMed: 19732329]

94. Takazawa T, Nishikawa K, Watanabe I, Goto F. Preoperative evaluation of hemodynamics using indocyanine green clearance meter in patients with peritonitis from gastrointestinal perforation. Masui. 2005; 54:260–4. [PubMed: 15794102]

95. Hoff R, Rinkel G, Verweij B, Algra A, Kalkman C. Blood volume measurement to guide fluid therapy after aneurysmal subarachnoid hemorrhage: a prospective controlled study. Stroke. 2009; 40:2575–7. [PubMed: 19423854]

96. Okochi O, Kaneko T, Sugimoto H, Inoue S, Takeda S, Nakao A. ICG pulse spectrophotometry for perioperative liver function in hepatectomy. J Surg Res. 2002; 103:109–13. [PubMed: 11855925]

97. Nagano K, Kusaka T, Okubo K, Yasuda S, Okada H, Namba M, Kawada K, Imai T, Isobe K, Itoh S. Estimation of circulating blood volume in infants using the pulse dye densitometry method. Paediatr Anaesth. 2005; 15:125–30. [PubMed: 15675929]

98. Bradley EC, Barr JW. Determination of blood volume using indocyanine green (cardio-green) dye. Life Sci. 1968; 7:1001–7. [PubMed: 4898425]

99. Fukuda H, Kawamoto M, Yuge O. A comparison of finger and nose probes in pulse dye-densitometry measurements of cardiac output, blood volume and mean transit time. Masui. 2001; 50:1351–6. [PubMed: 11797366]

100. Iijima T, Aoyagi T, Iwao Y, Masuda J, Fuse M, Kobayashi N, Sankawa H. Cardiac output and circulating blood volume analysis by pulse dye-densitometry. J Clin Monit. 1997; 13:81–9. [PubMed: 9112203]

101. Iijima T, Iwao Y, Sankawa H. Circulating blood volume measured by pulse dye- densitometry: comparison with (131)I-HSA analysis. Anesthesiology. 1998; 89:1329–35. [PubMed: 9856706]

102. Ikarashi A, Nogawa M, Yamakoshi T, Tanaka S, Yamakoshi K. An optimal spot-electrodes array for electrical impedance cardiography through determination of impedance mapping of a regional area along the medial line on the thorax. Conf Proc IEEE Eng Med Biol Soc. 2006; 1:3202–5. [PubMed: 17947015]

103. Kasuya Y, Kawai H, Yamamoto T, Dohi S. Comparison of pulse dye densitometry and thermodilution method in cardiac output measurement. Masui. 1998; 47:756–8. [PubMed: 9691601]

104. Sakka SG, Reinhart K, Wegscheider K, Meier-Hellmann A. Comparison of cardiac output and circulatory blood volumes by transpulmonary thermo-dye dilution and transcutaneous indocyanine green measurement in critically ill patients. Chest. 2002; 121:559–65. [PubMed: 11834672]

105. Tichy JA, Loucka M, Trefny ZM, Hojerova M, Svacinka J, Muller J, Friedrichova M. New clearance evaluation method for hepatological diagnostics. Physiol Res. 2009; 58:287–92. [PubMed: 17949250]

106. Hofer CK, Ganter MT, Zollinger A. What technique should I use to measure cardiac output? Curr Opin Crit Care. 2007; 13:308–17. [PubMed: 17468564]

107. Bremer F, Schiele A, Tschaikowsky K. Cardiac output measurement by pulse dye densitometry: a comparison with the Fick's principle and thermodilution method. Intensive Care Med. 2002; 28:399–405. [PubMed: 11967592]

108. Mock DM, Mock NI, Lankford GL, Burmeister LF, Strauss RG, Widness JA. Red cell volume can be accurately determined in sheep using a nonradioactive biotin label. Pediatr Res. 2008; 64:528–32. [PubMed: 18596580]

109. Mock DM, Matthews NI, Strauss RG, Burmeister LF, Schmidt R, Widness JA. Red blood cell volume can be independently determined in vitro using sheep and human red blood cells labeled at different densities of biotin. Transfusion. 2009; 49:1178–85. [PubMed: 19220818]

110. Mock DM, Matthews NI, Zhu S, Burmeister LF, Zimmerman MB, Strauss RG, Schmidt RL, Nalbant D, Freise KJ, Veng-Pedersen P, et al. Red blood cell (RBC) volume can be independently determined in vivo in the sheep using ovine RBCs labeled at different densities of biotin. Transfusion. 2010

111. Mock DM, Matthews NI, Zhu S, Burmeister LF, Zimmerman MB, Strauss RG, Schmidt RL, Nalbant D, Cress GA, Widness JA. Red blood cell (RBC) volume can be independently determined in vivo in humans using RBCs labeled at different densities of biotin. Transfusion. 2010

112. Mock DM, Matthews NI, Zhu S, Strauss RG, Schmidt RL, Nalbant D, Cress GA, Widness JA. Erythrocyte survival determined in humans using red blood cells labeled at multiple biotin densities. Transfusion. 2010 in press.
113. Wang LV. Multiscale photoacoustic microscopy and computed tomography. Nat Photonics. 2009; 3:503–509. [PubMed: 20161535]
114. Wang, WL., editor. Photoacoustic imaging and spectroscopy. N.Y.: Taylor & Francis/CRC Press; 2009.
115. Razansky D, Distel M, Vinegoni C, Ma R, Perrimon N, Koster RW, Ntziachristos V. Multispectral opto-acoustic tomography of deep-seated fluorescent proteins in vivo. Nat Photon. 2009; 3:412–417.
116. Mallidi S, Larson T, Tam J, Joshi PP, Karpiouk A, Sokolov K, Emelianov S. Multiwavelength photoacoustic imaging and plasmon resonance coupling of gold nanoparticles for selective detection of cancer. Nano Lett. 2009; 9:2825–31. [PubMed: 19572747]
117. Shashkov EV, Everts M, Galanzha EI, Zharov VP. Quantum dots as multimodal photoacoustic and photothermal contrast agents. Nano Lett. 2008; 8:3953–8. [PubMed: 18834183]
118. Modestov VK, Shul'tsev GP, Kulakov GP, Gavrilova GA. Radioisotope renography and kidney scanning in nephrologic and urologic diseases. Ter Arkh. 1969; 41:88–94. [PubMed: 5364566]
119. Modestov AD, Pleskov YV, Varnin VP, Teremetskaya IG. Synthetic semiconductor diamond electrodes: A study of electrochemical activity in a redox system solution. Russian Journal of Electrochemistry. 1997; 33:55–60.
120. Harada M, Shibata M, Kitamori T, Sawada T. Application of coaxial beam photothermal microscopy to the analysis of a single biological cell in water. Analytica Chimica Acta. 1995; 299:343–347.
121. Tokeshi M, Uchida M, Hibara A, Sawada T, Kitamori T. Determination of subyoctomole amounts of nonfluorescent molecules using a thermal lens microscope: subsingle-molecule determination. Anal Chem. 2001; 73:2112–6. [PubMed: 11354498]
122. Ermilov, S.; Stein, A.; Conjusteau, A.; Gharieb, R.; Lacewell, R.; Miller, T.; Thompson, S.; Otto, P.; McCorvey, B.; Khamapirad, T., et al. Detection and noninvasive diagnostics of breast cancer with 2-color laser optoacoustic imaging system. Oraevsky, AA.; Wang, LV., editors. San Jose, CA, USA: SPIE; 2007. p. 643703-11.
123. Vaartjes, SE.; van Hespen, JCG.; Klaase, JM.; van den Engh, FM.; The, AKH.; Steenbergen, W.; van Leeuwen, TG.; Manohar, S. First clinical trials of the Twente photoacoustic mammoscope (PAM). Pogue, BW.; Cubeddu, R., editors. Munich, Germany: SPIE; 2007. p. 662917-12.
124. Petrov YY, Petrova IY, Patrikeev IA, Esenaliev RO, Prough DS. Multiwavelength optoacoustic system for noninvasive monitoring of cerebral venous oxygenation: a pilot clinical test in the internal jugular vein. Opt Lett. 2006; 31:1827–9. [PubMed: 16729084]
125. Petrova IY, Esenaliev RO, Petrov YY, Brecht HP, Svensen CH, Olsson J, Deyo DJ, Prough DS. Optoacoustic monitoring of blood hemoglobin concentration: a pilot clinical study. Opt Lett. 2005; 30:1677–9. [PubMed: 16075535]
126. Yaseen MA, Yu J, Jung B, Wong MS, Anvari B. Biodistribution of encapsulated indocyanine green in healthy mice. Mol Pharm. 2009; 6:1321–32. [PubMed: 19799463]
127. Saxena V, Sadoqi M, Shao J. Enhanced photo-stability, thermal-stability and aqueous-stability of indocyanine green in polymeric nanoparticulate systems. J Photochem Photobiol B. 2004; 74:29–38. [PubMed: 15043844]
128. Shestakov NM. Complexity and inadequacy of current methods of determining circulating blood volume and the feasibility of a simpler and faster method of determining it. Ter Arkh. 1977; 49:115–20. [PubMed: 860244]
129. Tsopelas C, Sutton R. Why certain dyes are useful for localizing the sentinel lymph node. J Nucl Med. 2002; 43:1377–82. [PubMed: 12368377]
130. Dawson AB, Evans HM, Whipple GH. BLOOD VOLUME STUDIES: III. Behavior of Large Series of Dyes Introduced into the Circulating Blood. Am J Physiol. 1920; 51:232–256.
131. Shoemaker K, Rubin J, Zumbro GL, Tackett R. Evans blue and gentian violet: alternatives to methylene blue as a surgical marker dye. J Thorac Cardiovasc Surg. 1996; 112:542–4. [PubMed: 8751527]

132. Tarazi RC. Chapter 8: Blood Volume. European Heart Journal. 1985; 6:41–42. [PubMed: 4076224]

133. Gregersen MI, Rawson RA. Blood Volume. Physiological Reviews. 1959; 39:307–342. [PubMed: 13645237]

134. Riley AA, Arakawa Y, Worley S, Duncan BW, Fukamachi K. Circulating blood volumes: a review of measurement techniques and a meta-analysis in children. ASAIO J. 2010; 56:260–4. [PubMed: 20335800]

135. Wennesland R, Brown E, Hopper J Jr, Hodges JL Jr, Guttentag OE, Scott KG, Tucker IN, Bradley B. Red cell, plasma and blood volume in healthy men measured by radiochromium (Cr51) cell tagging and hematocrit: influence of age, somatotype and habits of physical activity on the variance after regression of volumes to height and weight combined. J Clin Invest. 1959; 38:1065–77. [PubMed: 13664782]

136. Brown E, Hopper J Jr, Hodges JL Jr, Bradley B, Wennesland R, Yamauchi H. Red cell, plasma, and blood volume in the healthy women measured by radiochromium cell-labeling and hematocrit. J Clin Invest. 1962; 41:2182–90. [PubMed: 14015940]

137. Karpinska J, Sokol A, Rozko M. Applicability of Derivative Spectrophotometry, Bivariate Calibration Algorithm, and the Vierordt Method for Simultaneous Determination of Ranitidine and Amoxicillin in Their Binary Mixtures. Analytical Letters. 2009; 42:1203–1218.

138. Dinc E, Onur F. Comparative study of the ratio spectra derivative spectrophotometry, derivative spectrophotometry and Vierordt's method applied to the analysis of oxfendazole and oxyclozanide in a veterinary formulation. Analusis. 1997; 25:55–59.

139. Schmidt W. A high performance micro-dual-wavelength-spectrophotometer (MDWS). J Biochem Biophys Methods. 2004; 58:15–24. [PubMed: 14597185]

140. Smirnova A, Proskurnin MA, Bendrysheva SN, Nedosekin DA, Hibara A, Kitamori T. Thermooptical detection in microchips: from macro- to micro-scale with enhanced analytical parameters. Electrophoresis. 2008; 29:2741–53. [PubMed: 18546176]

141. Petrova I, Prough D, Petrov Y, Brecht HP, Svensen C, Olsson J, Deyo D, Esenaliev R. Optoacoustic technique for continuous, noninvasive measurement of total hemoglobin concentration: an in vivo study. Conf Proc IEEE Eng Med Biol Soc. 2004; 3:2059–61. [PubMed: 17272125]

142. Sethi PD, Chatterjee PK, Jain CL. Spectrophotometric assays of diloxanide furoate and tinidazole in combined dosage forms. J Pharm Biomed Anal. 1988; 6:253–8. [PubMed: 16867415]

143. Elsayed L, Hassan SM, Kelani KM, El-Fatatry HM. Simultaneous spectrophotometric determination of nifuroxime and furazolidone in pharmaceutical preparations. J Assoc Off Anal Chem. 1980; 63:992–5. [PubMed: 6447688]

144. Hassan SM, Belal F, Sultan M. Simultaneous spectrophotometric determination of furazolidone and berberine in tablet form. Talanta. 1988; 35:977–80. [PubMed: 18964659]

145. Hofschulte B. The establishment and closure of the Veterinary School in Karlsruhe. Hist Med Vet. 1999; 24:84–7. [PubMed: 11623944]

146. Banoglu E, Ozkan Y, Atay O. Dissolution tests of benazepril-HCl and hydrochlorothiazide in commercial tablets: comparison of spectroscopic and high performance liquid chromatography methods. Farmaco. 2000; 55:477–83. [PubMed: 11204749]

147. Brusnichkin A, Nedosekin D, Ryndina E, Proskurnin M, Gleb E, Lapotko D, Vladimirov Y, Zharov V. Determination of various hemoglobin species with thermal-lens spectrometry. Moscow University Chemistry Bulletin. 2009; 64:45–54.

148. Proskurnin MA, Abroskin AG, Yu D, Radushkevich DY. A dual-beam thermal lens spectrometer for flow analysis. Journal of Analytical Chemistry. 1999; 54:91–97.

149. Bialkowski, SE. Photothermal spectroscopy methods for chemical analysis. Winefordner, JD., editor. New York: A Wiley-Interscience publication; 1996. p. 584

150. Proskurnin MA, Abroskin AG. Optimization of optical system parameters in dual-beam thermal lens spectrometry. Journal of Analytical Chemistry. 1999; 54:401–408.

151. Zhidkova TV, Proskurnin MA, Sokolov ME, Polenova TV, Ivanova EK. Spectrophotmetric rapid estimation of circulating blood volume without *a priori* data. Tekhnologii Zhivykh Sistem. 2010:26–34.

152. Svehla G. Differential spectrophotometry. Talanta. 1966; 13:641–66. [PubMed: 18959926]
153. Gorelik AI, Mokhova EN. Differential spectrophotometry of biological objects characterized by strong light diffusion. Nauchnye Doki Vyss Shkoly Biol Nauki. 1976:137–44. [PubMed: 1026262]
154. Ku G, Wang LV. Deeply penetrating photoacoustic tomography in biological tissues enhanced with an optical contrast agent. Opt Lett. 2005; 30:507–9. [PubMed: 15789718]
155. Wei X, Runnels JM, Lin CP. Selective uptake of indocyanine green by reticulocytes in circulation. Invest Ophthalmol Vis Sci. 2003; 44:4489–96. [PubMed: 14507897]
156. Yong WH, Mattia AR, Ferraro MJ. Comparison of fecal lactoferrin latex agglutination assay and methylene blue microscopy for detection of fecal leukocytes in Clostridium difficile-associated disease. J Clin Microbiol. 1994; 32:1360–1. [PubMed: 8051268]
157. Noltingwj DE. Quantitative Determination of the Impregnation of Methylene Blue in Leukocytes. Geneeskd Gids. 1964; 42:45–7. [PubMed: 14144656]
158. Strober W. Trypan blue exclusion test of cell viability. Curr Protoc Immunol. 2001 Appendix 3:Appendix 3B.
159. Tennant JR. Evaluation of the Trypan Blue Technique for Determination of Cell Viability. Transplantation. 1964; 2:685–94. [PubMed: 14224649]
160. Zijlstra, WG.; Buursma, A.; van Assendelft, OW. Visible and near infrared absorption spectra of human and animal haemoglobin. Utrecht: VSP; 2000. p. 368

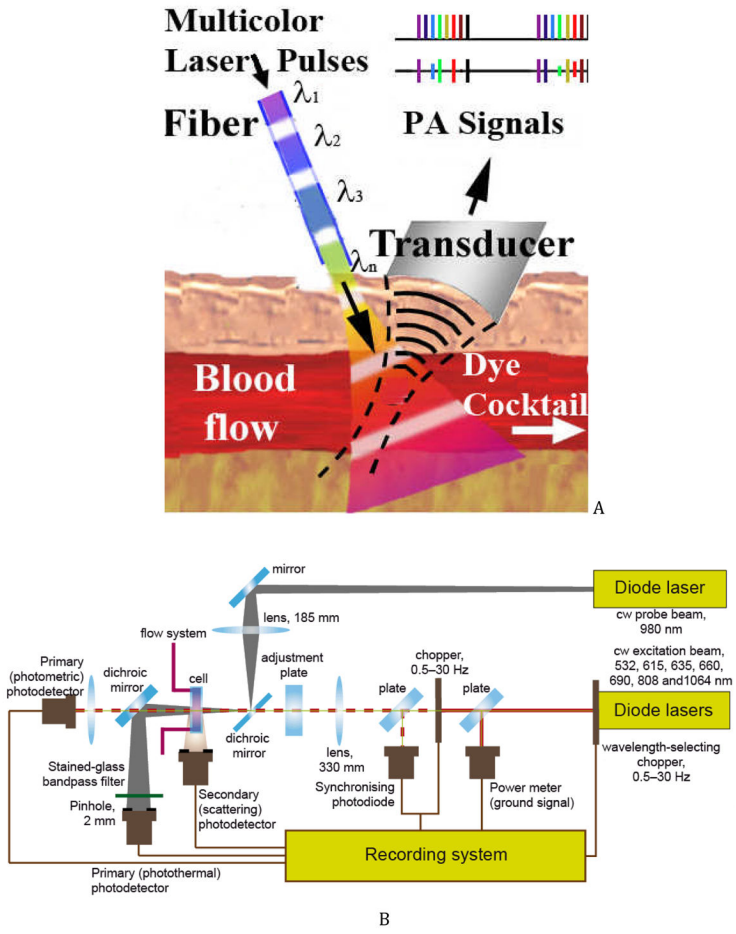

Fig. 1.

The principle of multispectral photoacoustic flow cytometry with multicolor dyes (a) and schematics of photothermal measurements used in the study (b).

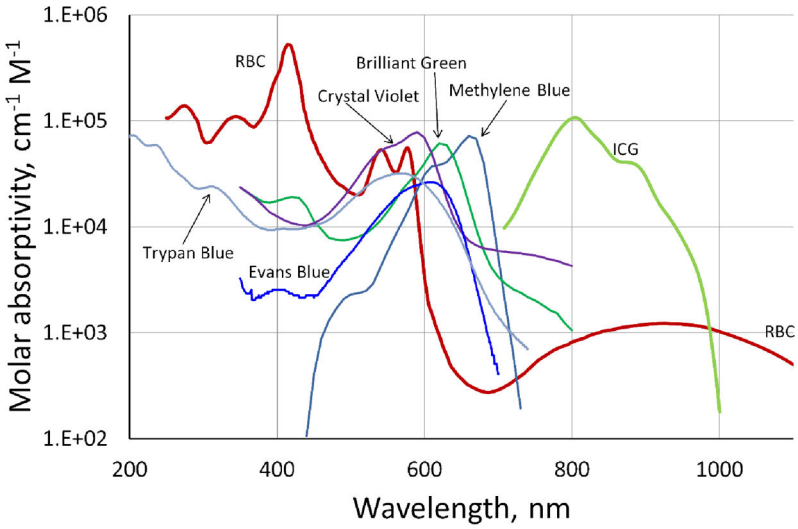

Fig. 2.
Molar absorption spectra of oxygenated RBCs (160) and several dyes selected for this study.

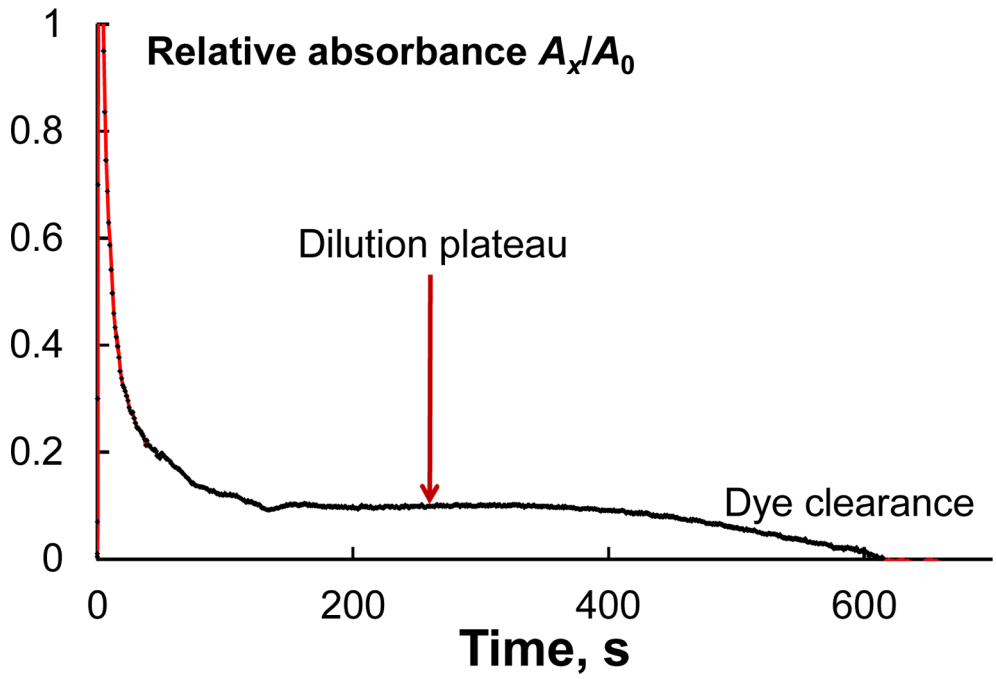

Fig. 3.

The dilution curve of ICG in PT CBV measurements at 808 nm (after the subtraction of blood background). *A* is PT signal amplitude. The dilution plateau results from a combination of immediate dilution in the circulation followed by later hepatic clearance. CBV is estimated from the plateau.

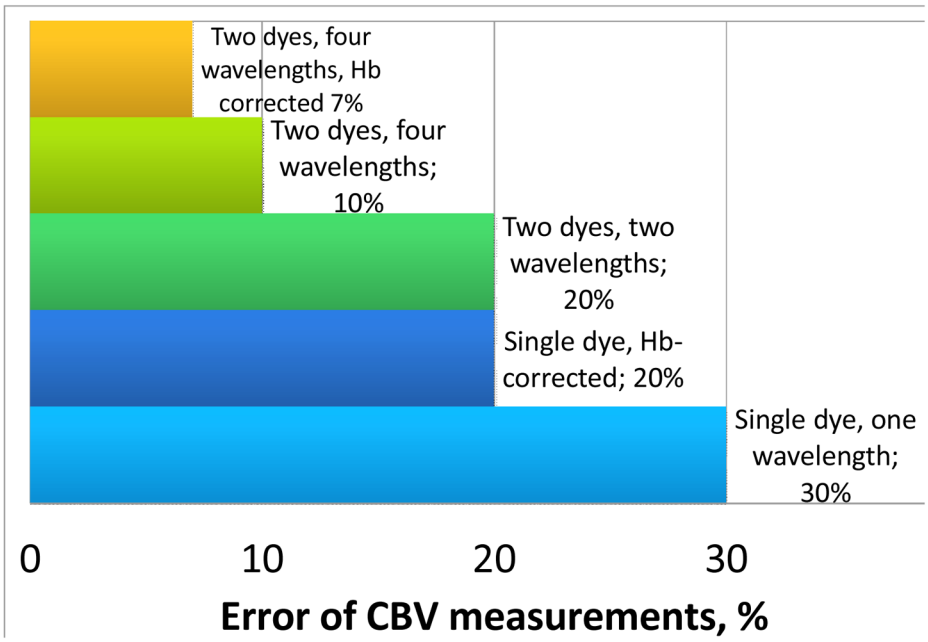

Fig. 4.

Modeling of CBV measurement error depending on the selection of the dye mixture (ICG + Methylene Blue) and the correction for [Hb].

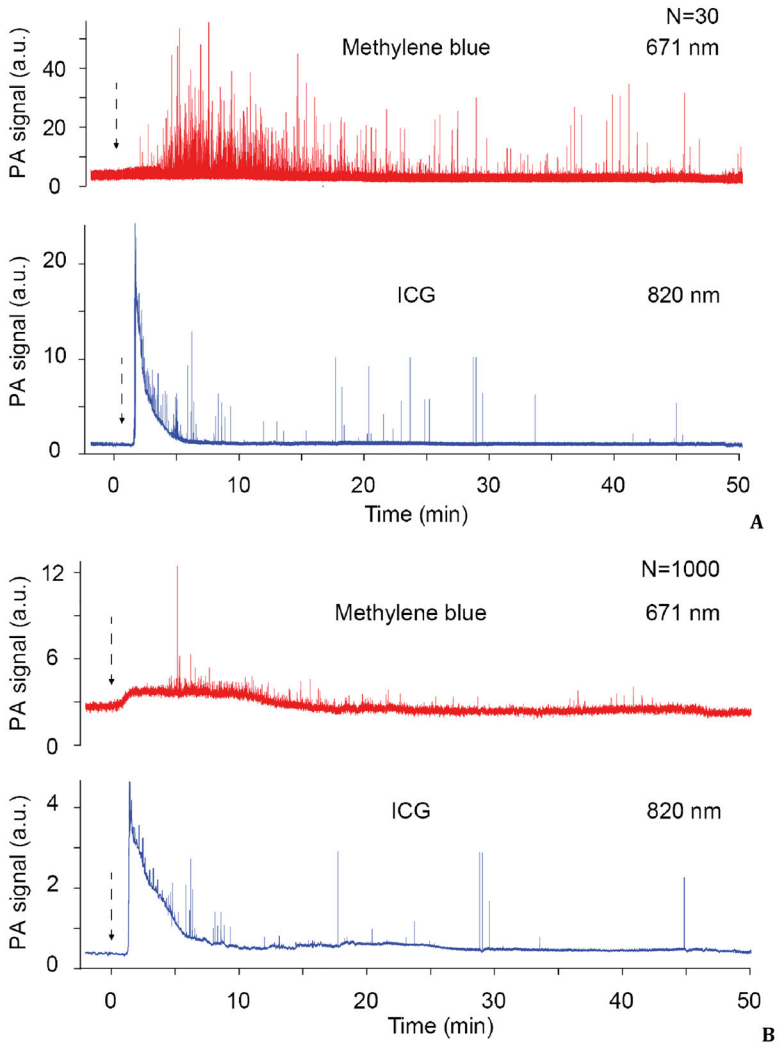

Fig. 5.

In vivo photoacoustic monitoring of clearance rate simultaneously for two dyes in mouse ear microvessels at different signal averaging $N = 30$ (A) and $N = 1000$ (B). Laser parameters: pulse rate, 10 kHz; energy fluence, 50 mJ/cm^2.

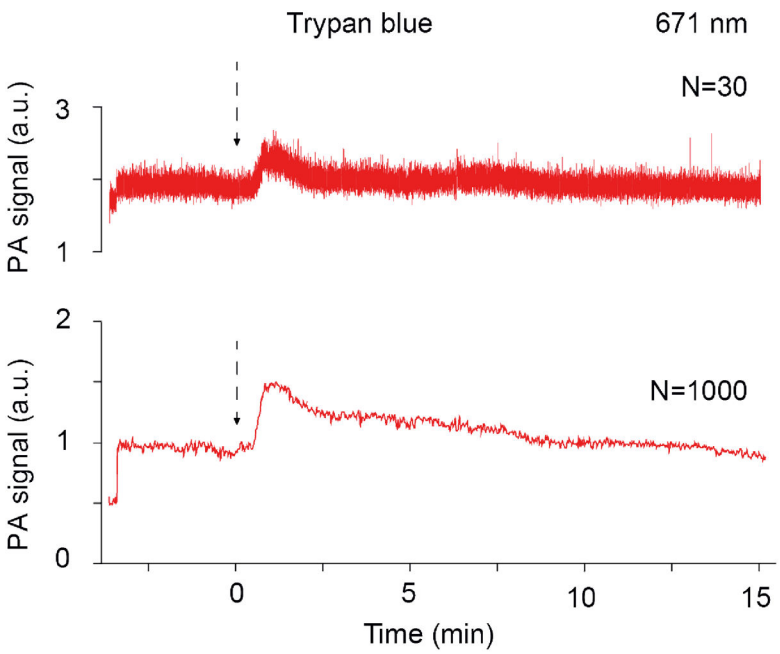

Fig. 6.

In vivo photoacoustic monitoring of clearance rate of Trypan Blue (TB) at different signal averaging (N = 30, and N = 1000). Laser parameters: wavelength, 671 nm; pulse rate, 10 kHz; energy fluence, 50 mJ/cm^2.

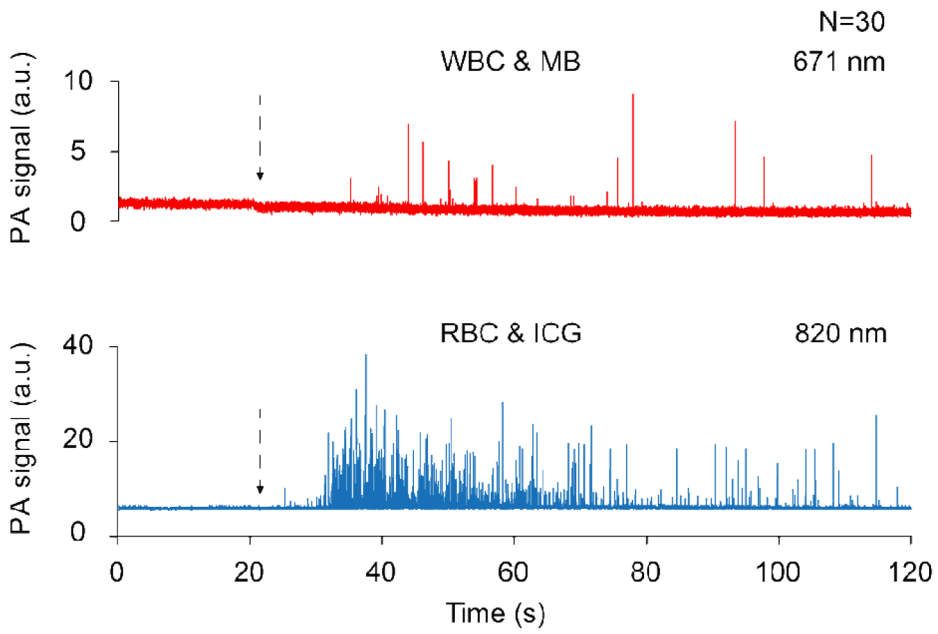

Fig. 7.

In vivo photoacoustic monitoring of circulating WBCs and RBCs labeled priory in vitro with MB, and ICG, respectively. Laser parameters: wavelengths, 671 nm and 820 nm, pulse rate, 10 kHz; energy fluence, 50 mJ/cm^2

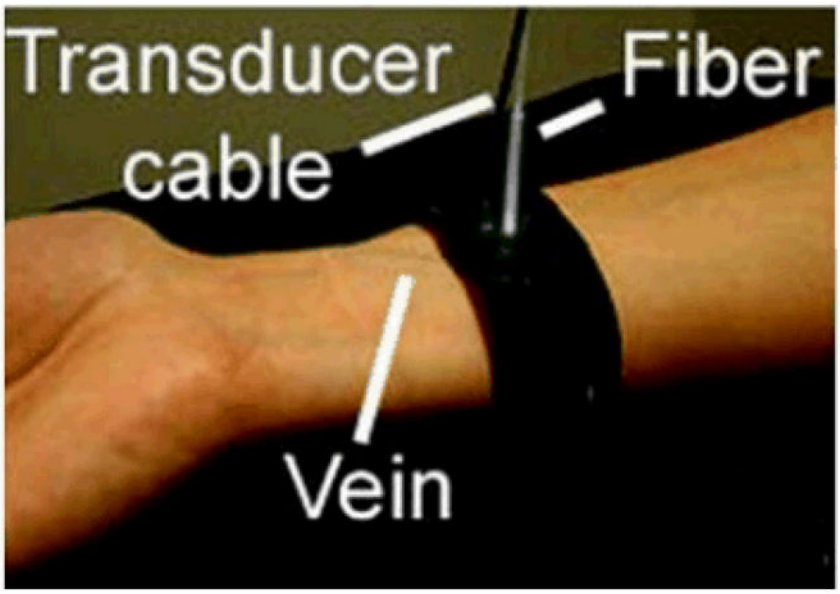

Fig. 8.
Clinical prototype of an *in vivo* photoacoustic flow cytometer.

Table

Parameters of determination of Methylene Blue (MB), Crystal Violet (CV), and Indocyanine Green (ICG) at dual wavelengths and four-wavelength measurements of their dual mixtures (cocktails) in blood (blood absorption was corrected at 532 and 1064 nm), $n = 5$, $P = 0.95$

Dye or dual mixture	λ, nm	Optical detection			PT detection			
		$c_{min}\times10^6$ M	Linear calibration range $\times10^5$ M	r	$c_{min}\times10^8$ M	Linear calibration range $\times10^7$ M	r	RSD of CBV determination, %
MB	635 + 690	10	4–20	0.9896	20	5–400	0.9733	15
	635 + 660	10		0.9268	20		0.9354	20
CV	610 + 690	2	3–20	0.9766	5	8–500	0.9811	20
	610 + 660	2		0.9726	5		0.9900	25
	635 + 690	3		0.9897	7		0.9635	20
	635 + 660	3		0.9857	6		0.9759	20
ICG	690 + 808	1	3–30	0.9765	1	3–300	0.9960	15
	660 + 808	1		0.9856	1		0.9945	15
MB + CV	610 + 635 + 660 +690	10/3*	3–30	0.9654	30/1	5–400	0.9320	6
MB + ICG	635 + 660 +690 + 808	20/1	3–30	0.9529	30/2	5–400	0.9425	7
CV + ICG	610 + 660 +690 + 808	3/1	3–30	0.9348	5/2	5–400	0.9239	7

Remark:

* Limits of detection correspond to the first/second component of a dual mixture